ARMA e-NEWSLETTER 18

AMERICAN ROCK MECHANICS ASSOCIATION • ISSUE 18 • SPRING 2016

In this issue

Invitation to Houston:

50th US ROCK MECHANICS/ GEOMECHANICS SYMPOSIUM

26-29 June 2016

The American Rock Mechanics Association (ARMA) invites you to its 50th US Rock Mechanics/Geomechanics Symposium to be held in Houston, Texas, USA on 26-29 June 2016. The symposium's technical committee, led by symposium chair David Yale, selected almost 400 papers from 717 abstracts submitted. Forty-eight technical sessions and two poster sessions are planned over three full days. The sessions will focus on petroleum engineering, mining engineering, civil and environmental engineering, and interdisciplinary topics (see below for subject areas). Eighteen companies and organizations are exhibiting.

As with previous symposia, we have also lined up world-renowned scientists to give a series of keynote addresses that highlight the importance and impact of geomechanics and rock mechanics. Keynote speakers include the MTS Lecture by Peter Kaiser and ARMA's first Distinguished Lecture by Richard Goodman. William Ellsworth, Jean-Claude Roegiers, and Charles Fairhurst round out the keynote addresses. Technical tours have been arranged highlighting Houston's petroleum history (tours to Spindletop and the Ocean Star Offshore Drilling Rig) and geology (tour on Active Faults in the Houston area).

(continued on page 2)

Two short courses are offered:

- Shale Gas GeoEngineering by Maurice Dusseault, Professor, Geological Engineering, University of Waterloo, Ontario, Canada; and
- Modeling of Coupled Hydro-Mechanical Deformation and Fracturing Processes in Geomechanics by Omid Mahabadi and Andrea Lisjak, Geomechanica, Inc.

Six workshops are included:

- ARMA/AAPG SedHeat Workshop on Successful Engineering of Sedimentary Geothermal Systems;
- Workshop on Hydraulic Fracturing;
- Geomechanics in Unconventionals Workshop for Asset Teams;
- How Laboratory Geomechanics Testing Adds Value to Exploration and Production;
- Microseismic Geomechanics from Laboratory to Field Scale Across All Industries; and
- ARMA Future Leaders/Students Open Discussion: "What's Your Problem?"

The symposium will be held in Houston at the Westin Galleria Hotel and Conference Center. Holding the meeting in Houston will allow a larger number of petroleum-related geomechanics professionals to attend and broaden the interaction between the rock mechanics/ geomechanics disciplines and industries. The Westin's Conference Center allows the symposium a breadth of space that should enhance networking opportunities with exhibitors, as well as allow an expanded and more interactive series of poster sessions. For further information on the program, other activities, or to register, please visit the symposium website: *http://armasymposium.org/*

Technical Session Subject Areas

Depletion Induced Surface Subsidence
Hazards, Risks, and Induced Seismicity
Induced/Triggered Seismicity
Waste Disposal and CO_2 Sequestration
Slope Stability, Foundation, and Dams
Underground Storage and Structures
Coupled Process
Drilling Geomechanics
Hydraulic Fracturing Case Studies
Integrated Reservoir Geomechanics
Interaction of Induced and Natural Fractures
Near-wellbore Processes
Sand Control and Management
Subsurface Stress Modification
Coal Mining Ground Control
Mining Geomechanics
Numerical Modeling in Mining
Rock Excavation, Breaking, Dynamic Loading
Rock Properties for Underground Excavation
Slope Stability in Mines
Computational Advances in Geomechanics
DFN Fracture Characterization
Fracture Modeling
Fracturing Mechanics
Geology in Geomechanics
Geomechanics in Geothermal Processes
Geophysics in Geomechanics
In Situ Stress and Pore Pressure
Interdisciplinary Topics
Laboratory and Field Measurements
Modeling Rock Mass Fracturing Process
Numerical Modeling
Numerical/Analytical/DEM Modeling
Rock Heterogeneity across Length Scales
Rock Characterization
Subsurface Integrity

Organizing Committee

David Yale, ExxonMobil (Ret.)
Joe Carvalho, Golder Associates, Inc.
John Kemeny, University of Arizona
Doug Blankenship, Sandia National Labs
Doug Stead, Simon Fraser University
Sherlyn Williams-Stroud, CA Resources
Karim Zaki, Chevron Energy Technology
Azra N. Tutuncu, Colorado School of Mines
Andrew Bunger, University of Pittsburgh
Colleen Barton, Baker-Hughes
Ahmad Ghassemi, University of Oklahoma
Gang Han, Aramco Services Company
Ellen Mallman, BP
Edward Wellman, SRK Consulting
Kate Baker, ARMA Board
John Curran, ARMA Treasurer
Peter Smeallie, ARMA Executive Director

Case History

Parking Ramp Construction over the LRT Station Minneapolis-St. Paul International Airport

Submitted by Derrick Blanksma, Lauriane Bouzeran, Tryana Garza-Cruz, and Lee Petersen; Itasca Consulting Group, Inc., Minneapolis, MN

1.0 Introduction

Minneapolis-St. Paul International Airport (MSP) serves about 36 million passengers annually, via about 405,000 flight operations. On-airport parking provides about 22,900 parking spaces and is frequently at or near capacity. As a result, design is underway for a parking ramp expansion at Terminal 1-Lindbergh. The facility is served by the Metro Transit light-rail (LRT) Blue Line. The existing LRT station is underground and adjacent to the existing parking ramp. The proposed parking ramp expansion will be constructed over the north end of the LRT station. As illustrated in Figure 1, the LRT station is constructed in an excavation in the St. Peter sandstone and Glenwood shale, with a flat roof of the Platteville limestone. Excavation dimensions are about 55 feet wide by 40 feet high by 540 feet long. The station is shallow, with the bottom of the Platteville limestone approximately 30 feet below the existing revenue control plaza for on-airport parking, which is located above the station.

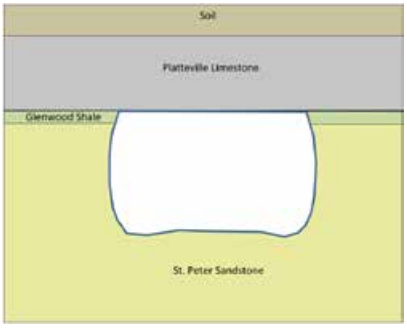

Figure 1. Geologic cross-section at the LRT station.

Construction of the parking ramp expansion involves two principal impacts on the LRT station: a) column loads on the Platteville limestone above or nearby the station; and b) excavation of the soil cover and some of the Platteville limestone above the station. As part of the feasibility study described below, the magnitude of these impacts was assessed by conducting a 3D geostructural analysis of the station using Itasca's distinct element modeling software called *3DEC*.

3DEC is a numerical modeling software for advanced engineering analysis of soil, rock, blocky structures, and structural support in three dimensions. *3DEC* simulates the response of discontinuous media (such as jointed rock or masonry structures) that are subject to either static or dynamic loading. A discontinuous medium is modeled as an assemblage of polyhedral blocks that may be rigid or made deformable through zoning. Fractures are treated as boundary conditions between blocks. Motion along discontinuities is governed by linear and nonlinear force-displacement relations for movements in both the normal and shear directions. *3DEC* uses an explicit solution that provides a realistic path-dependent post-peak failure behavior in joints and zones, as well as simulation of large displacements. The blocks may be rigid or deformable.

2.0 LRT Station Construction

The LRT station was constructed in 2002 and 2003 in coordination with excavation and lining of the TBM (tunnel boring machine) tunnels serving the station. The top heading was excavated incrementally from the north to the south end. As increments were excavated, the limestone roof was trimmed to remove the Glenwood shale. The roof was rockbolted using point-anchored, hollow Williams rockbolts. The rockbolts were tensioned at installation and later retensioned and cement-grouted. Additional resin-grouted threadbar rockbolts were added in response to measured roof deflections. The benches were excavated, and the station walls trimmed to receive precast concrete panels. Roof and wall trimming was done by a roadheader attachment on a track-mounted excavator. Figure 2 shows the state of the LRT station construction in April 2003.

The LRT station roof and wall behavior was monitored using surface survey points, inclinometers, and extensometers. The surface survey points and inclinometers were valuable in calibrating the *3DEC* model.

Figure 2. LRT station under construction.

3.0 Model Description

The *3DEC* structural model of the station included the excavation, station roof, adjacent subsurface materials, and adjacent existing structures (loads only). The model did not include the precast lining of the tunnel boring machine (TBM) tunnels, the precast wall panels in the station, the shotcrete end walls of the station, or the rockbolts located in the sandstone.

3.1 Geology

The *3DEC* model embodied the geologic layers, elevations, and thicknesses listed in Table 1. The two limestone layers were modeled with explicit bedding planes at elevations 789, 794, 797, and 801. The limestone layers also included explicit joints, as described in Section 3.2.

3.2 Limestone Jointing

Table 1. Model Geology

Geologic Layer	Layer Elevations (ft)	Layer Thickness (ft)
Soil	810.5–820.5	10
Upper Platteville Limestone	803.5–810.5	7
Lower Platteville Limestone	786.5–803.5	17
St. Peter Sandstone	620.5–786.5	166

Figure 3 is a plan view of the station, where north is up. The north shaft is at the northeast end of the station (upper right), the south shaft is at the southwest end of the station, and the Transit Center Connection is near the middle of the station. The joints in the limestone roof were characterized during station construction. The figure illustrates the location and nature of these limestone joints. All limestone joints are subvertical, and the following colors represent joints of different character:

1. Red: Limestone joint, greater than 1 gpm inflow.
2. Yellow: Limestone joint, open ⅛ inch to ¼ inch, drip to 1 gpm.
3. Green: Limestone joint, open 0 inch to ⅛ inch, dry to drip.

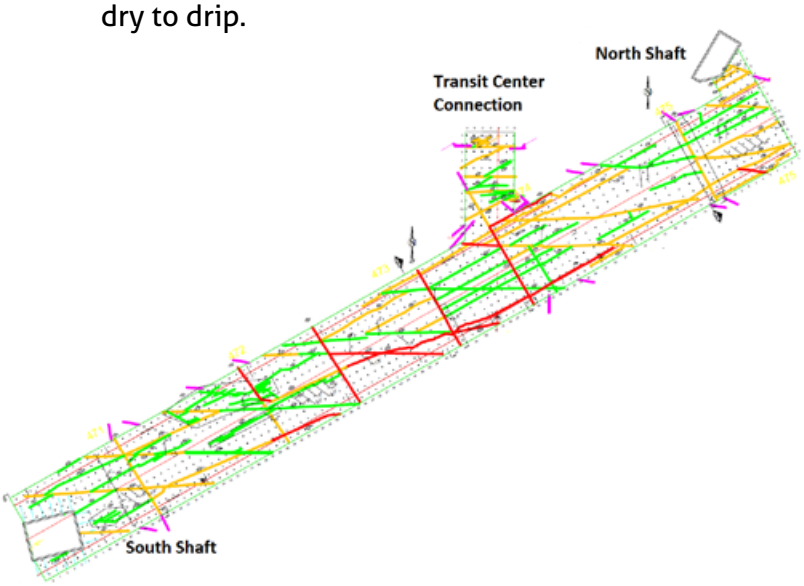

Figure 3. Platteville limestone joints mapped during construction.

The joints exhibit three preferred orientations, summarized in Table 2. Set A strikes northwest-southeast, and is essentially perpendicular to the station axis. As listed in Table 2, six joints from Set A were exposed during construction over the 530-ft length of the station. Hence, the average spacing is about 88 ft. Set B strikes east-west, and about 17 were exposed by station construction. (In Table 2, the exposure distance listed is the length of the station exposure perpendicular to the joint set strike.) Finally, Set C strikes northeast-southwest, is parallel to the station axis (perpendicular to Set A), and was encountered 12 times.

The 3DEC model extends beyond the station limits in order to provide boundary conditions that don't impact model behavior. Joints were mapped only within the station footprint, so a procedure was necessary to populate the remainder of the model with similar jointing. Hence, the 3DEC model incorporated the joint sets differently depending upon the set and location. Within the limits of the exposed station roof, the model contained the joints at the locations depicted in Figure 3. Outside the exposed station roof, all joints in sets A and B were extended to the full extent of the model. Outside the station, the joints in set C were generated randomly and were terminated at intersections with sets A and B.

Table 2. Summary of Mapped Joint Sets

Joint Set	Trend	No. of Joints in Each Set Encountered in Station Roof	Approximate Exposure Distance (ft) Perpendicular to Joint Set Strike	Average Spacing (ft)	Estimated Persistence
A	NW-SE	6	530	88	Hundreds of feet
B	E-W	17	300	18	Hundreds of feet
C	NE-SW	12	100	8	Hundreds of feet

4.0 Model Calibration

Model calibration was conducted by adjusting model parameters to approximately reproduce the measured performance of the station. The principal performance measurements of the station were settlement measurements on the surface above the station (typically referred to as the PK survey), horizontal deformations measured by vertical inclinometers, and observed behavior of the limestone and sandstone, including location and amount of sandstone sloughing. Initial runs were conducted using material properties based on 2D *FLAC* modeling conducted during station original construction.

4.1 Material Properties

4.1.1 Base Case

The base case material properties used in the models are shown in Table 3. The base case limestone joint and bedding plane material properties are shown in Table 4.

The base case properties listed in the preceding tables produced an over estimate of the settlement measurements taken at the end of the original construction. The parametric study, described in Section 4.1.2, was designed to "stiffen" the model to reduce predicted settlement to more closely match the settlement measurements taken at the end of the original construction.

4.1.2 Parametric Study

Five model parameters were varied in order to bring the predicted settlements into the approximate range and shape of the settlement and inclinometer measurements. These parameters include the following.

1. Limestone Young's modulus: Model runs were made with upper and lower limestone modulus two, three, and five times greater than the base case.

Table 3. Base Case Material Properties

Material	Unit Weight (pcf)	Young's Modulus (psi)	Poisson's Ratio	Cohesion (psi)	Friction Angle (deg)	Tensile Strength (psi)	Dilation Angle (deg)
Soil	115	3000	0.25	1	30	0	0
Upper limestone	165	20,000	0.2	333	30	33	10
Lower limestone	165	1e6	0.2	1000	40	100	10
Sandstone	125	3e5	0.2	100	50	10	10

Table 4. Base Case Joint and Bedding Plane Properties

Item	Normal Stiffness (lb/ft)	Shear Stiffness (lb/ft)	Cohesion (psi)	Friction Angle (deg)	Dilation Angle (deg)
Limestone joints	6.37e6	3.18e6	0	40	15
Bedding planes	6.37e5	3.18e5	10	30	0

2. Limestone bedding and joint stiffness: Model runs were made with both the lower limestone bedding and joint stiffness increased by a factor of 10.

3. Limestone bedding stiffness: Model runs were made with the lower limestone bedding stiffness increased by a factor of 10.

4. Limestone joint stiffness: Model runs were made with the lower limestone joint stiffness of selected joints increased by a factor of 5 or 10. In some runs, the stiffness of both green and yellow joints (see Figure 3) was increased by a factor of 10. In some runs, the green joint stiffness was increased by a factor of 10 and the yellow joint stiffness was increased by a factor of 5.

5. Rockbolt installation: The rockbolts were typically installed at 90 percent relaxation of the excavation, but in one run the rockbolts were installed at 50 percent relaxation.

4.2 Calibration Results

Three of the model runs described in Section 4.1.2 produced results that closely matched the measured settlements and deformations:

1. Case A: Limestone Young's modulus times 3, bedding plane stiffness times 10.

2. Case B: Limestone Young's modulus times 3, green joint stiffness times 10.

3. Case C: Limestone Young's modulus times 3, green joint stiffness times 10, yellow joint stiffness times 5.

These three cases were used in the feasibility analysis of design options.

5.0 Design Options

5.1 Option Description

Initially, two options were chosen for detailed 3DEC analysis: 1) application of the ramp column loads to the upper limestone over the station footprint; and 2) the use of transfer beams to carry all column loads outside the station footprint. Figure 4 illustrates the details of these two options, where the grid of black dots is the location of the planned columns. The amount and location of limestone excavation necessary also varied, and is illustrated by the red and green shaded areas. Ultimately, six options, illustrated in Figure 5, were chosen for detailed geostructural feasibility analysis. The figure shows the general concepts of the six options, but not the details. Major differences among the options are the amount of shallow limestone excavation necessary (shown shaded in red and green), the location and extent of transfer beams, and the amount of supplemental rockbolting. The six options were:

1. Option 1: Excavation of soil and upper limestone in areas as required to accommodate new infrastructure, with parking ramp column loads applied to the top of the remaining limestone.

2. Option 2: Excavation of revised (compared to Option 1) soil and upper limestone areas as required to accommodate new infrastructure, with parking ramp column loads carried by load transfer beams founded outside the station footprint.

3. Option 1' (Option 1 prime): This is Option 1 with additional station roof rockbolting installed prior to any excavation and application of ramp column loads.

4. Option 1A: This is a combination of Options 1 and 2. Column loads for the northernmost grid line are founded on the station roof, but the remaining column loads are carried by load transfer beams.

5. Option 1B: This is Option 1A with additional rockbolts in the north part of the station.

6. Option 1C: This is Option 1A with the center column on the northernmost grid line constructed through the limestone and founded in the sandstone. In the models, this option was modeled by eliminating the column load.

The magnitudes of column loads vary for all options and include both dead load from the structure, and transient loads from vehicles and wind loads imparted on the structure.

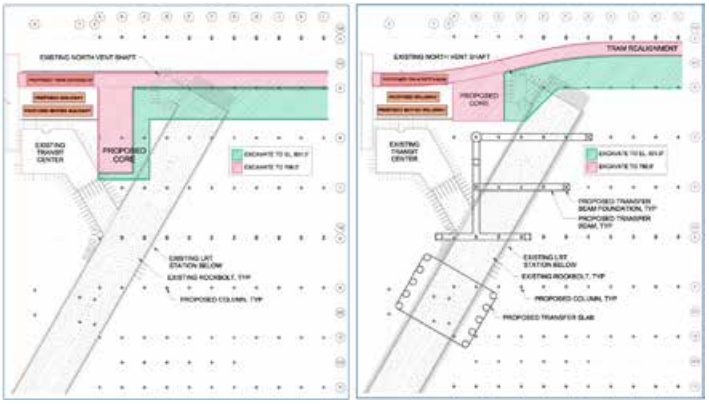

Figure 4. Layout of Option 1 (left) and Option 2 (right).

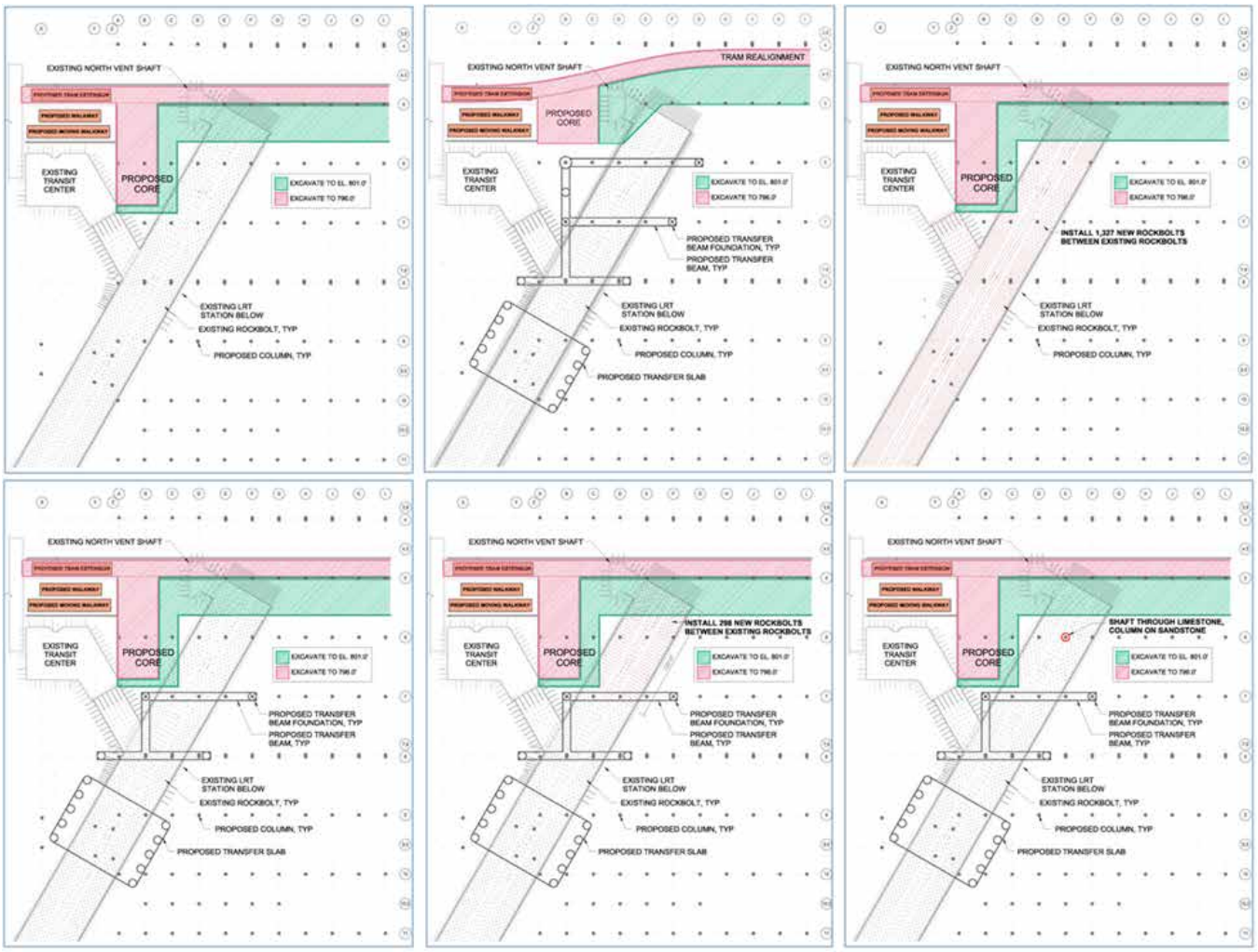

Figure 5. Layout of six options studied, top row left to right: Option 1, Option 2, Option 1'; bottom row left to right: Option 1A, Option 1B, Option 1C.

5.2 Effects on Joints and Bedding Planes

One measure of the feasibility of the various options is the factor of safety against slip for joints and bedding planes present in the Platteville limestone. Because all joints and bedding planes were modeled with Mohr-Coulomb strength limits, shear slip will occur whenever the shear stress exceeds the shear strength. Hence, the minimum possible factor of safety at any location will be one.

Figure 6 shows the factor of safety against slip for selected joints near the Transit Center connection to the LRT station. The plots are all for the current state of the station, prior to any excavation or column loads. Three plots are shown, because these are three independent analyses based on the material properties noted in Section 4.2, and the results are slightly different for each. However, the patterns of low factor of safety are similar for all three. Because the station

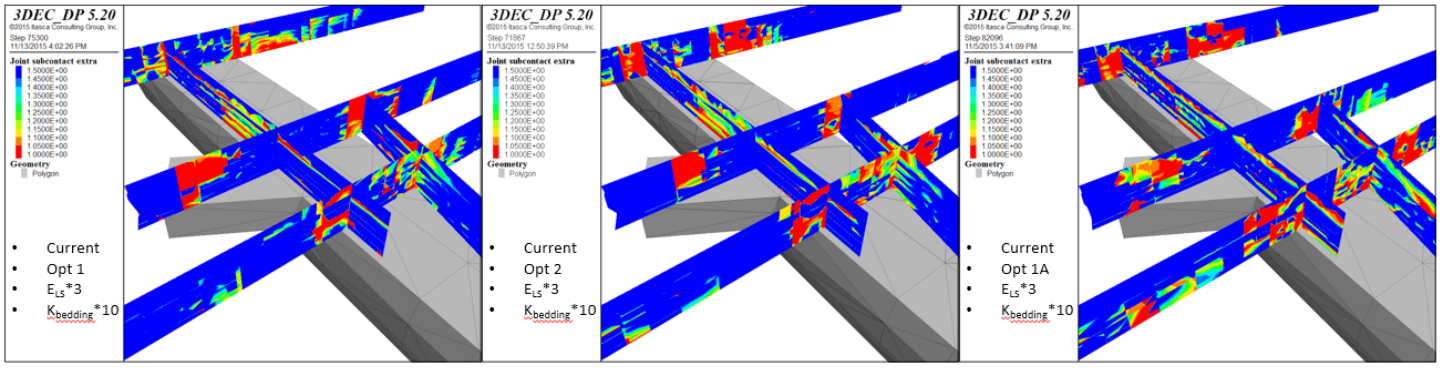

Figure 6. Predicted factor of safety against slip for selected vertical joints near the Transit Center connection for the current station state: Option 1 model (left); Option 2 model (center); and Option 1A model (right). (Red is FoS = 1.0 and blue is FoS>= 1.5.)

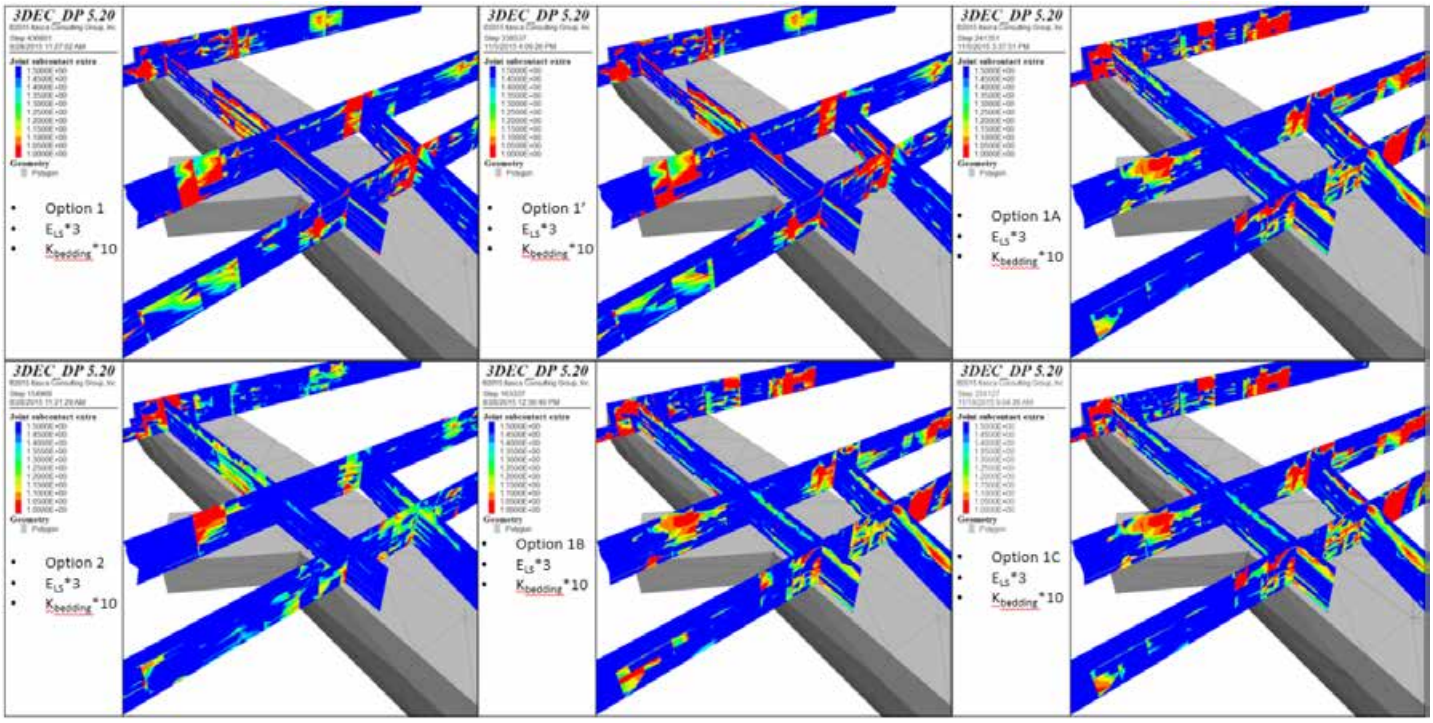

Figure 7. Predicted factor of safety against slip for selected vertical joints near the Transit Center connection after excavation and column loads: Option 1 model (upper left); Option 1' model (upper center); Option 1A model (upper right); Option 2 model (lower left); Option 1B model (lower center); and Option 1C model (lower right). (Red is FoS = 1.0 and blue is FoS>= 1.5.) [1]

is stable in the current state, the plots in this figure establish a base case against which to judge the impact of excavation and column loads. (Note that the other calibration cases have similar distributions of factor of safety.)

The impact of future excavation and column loads may be assessed by comparing the images in Figure 6 to the images in Figure 7. Although there are differences, excavation and application of column loads for the different design options does not produce large areas of low factor of safety on these joints. These figures illustrate that the vertical joints in the limestone have high factors of safety against slip for extensive regions. Future excavation and column loads do not appreciably affect the factors of safety. This finding shows that slip on vertical joints is not a likely mechanism leading to unacceptable behavior of the limestone roof of the station.

Figures 8 to 12 provide a comprehensive comparison of the predicted factor of safety for the four bedding planes included in the *3DEC* models. The bedding planes are at elevations 789, 794, 797, and 801 (4, 9, 12, and 16 ft above the roof). Figure **8** illustrates the predicted safety factor for the four bedding planes for the current state of the station. (All four plots are taken from the analysis of Option 1A.) Because the *3DEC* model has a Mohr-Coulomb strength criteria for all bedding planes and joints, the minimum possible safety factor is 1. Slip would occur for lower safety factors, bringing the location back to a safety factor of 1. The ten colors from red to blue are increments of 0.05 safety factor. All blue locations have a safety factor of 1.5 or above.

The plots in Figure 8 show that the rockbolts are effective at limiting the zones of low safety factor to locations roughly above the walls of the station.

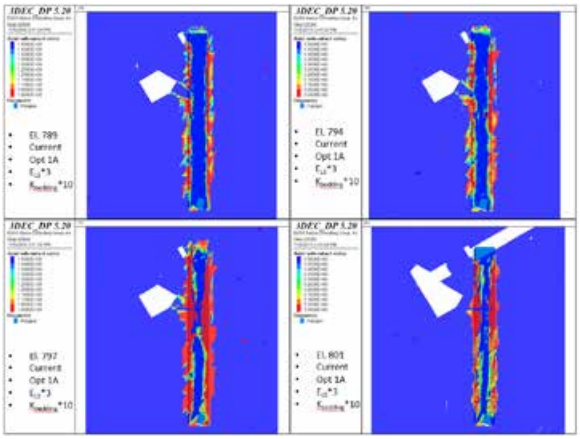

Figure 8. Predicted factor of safety against slip for the current station condition for the bedding planes at elevation 789 (upper left), 794 (upper right), 797 (lower left), and 801 (lower right).

[1]All FoS plots have the same scale: red is FoS = 1.0 and blue is FoS>= 1.5.

These are the locations where the thrust forces from the linear arches would be large. The limits of the low safety factor zones are also influenced by the vertical joints, producing the jagged outlines shown. The bedding planes at 797 and 801 are above the effective reach of the rockbolting, so they show broader zones of low safety factor.

Figures 9 - 12 show the safety factors for the bedding planes at 789, 794, 797, and 801, respectively, for all six options. (The specific calibration case chosen for the figures is Case A, described in Section 4.2, but other calibration cases are similar.) The general results described for the current state of the station in the preceding paragraph also occurs in these results: the rockbolts are effective at controlling the factor of safety for the 789 and 794 bedding planes, but are not effective for the higher bedding planes. Refer back to Figure 8 when reading the discussion of the other safety factor figures.

Rockbolting improves the safety factor against slip on bedding planes. Compare the upper left (Option 1) and upper middle (Option 1') plots in both Figure 9 and Figure 10. The extent of low safety factor (red areas) is significantly reduced. The same is true of the upper right (Option 1A) and lower middle (Option 1B) in the same figures.

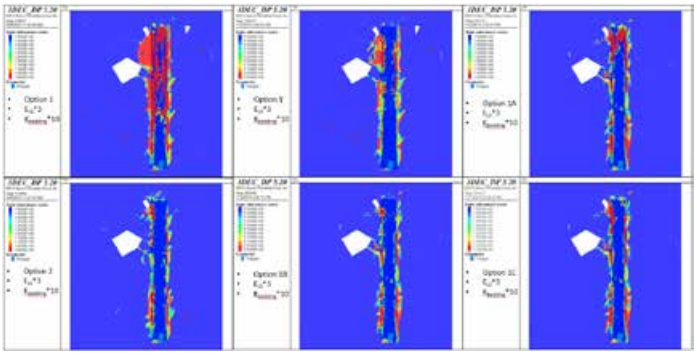

Figure 9. Predicted factor of safety against slip for the bedding plane at elevation 789: Option 1 model (upper left); Option 1' model (upper center); Option 1A model (upper right); Option 2 model (lower left); Option 1B model (lower center); and Option 1C model (lower right).

The conclusions listed below are based on the predicted amount of deflection (not discussed here due to space limitations), and the relative amount of low factor of safety regions present in the current state of the station (Figure 8) compared to the future options (Figures 9 to 12). For example, the upper right image in Figure 8 (which is for the bedding plane at elevation 794) was compared to the six images in Figure 10. Options with greater extent of low factor of safety, as compared to the current state, were considered undesirable, and options with lesser extent of low safety factor were considered desirable. This comparison is illustrated in Figure 13, where the red areas in the right image (Option 1) are substantially more extensive than in the left image (current condition).

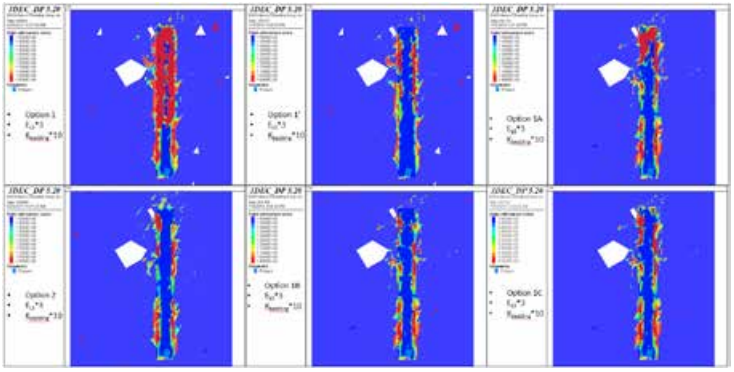

Figure 10. Predicted factor of safety against slip for bedding plane at elevation 794:Option 1 model (upper left); Option 1' (upper center); Option 1A (upper right); Option 2 (lower left); Option 1B (lower center); and Option 1C (lower right).

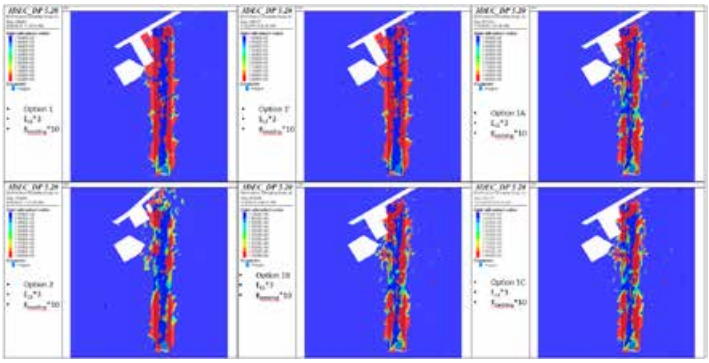

Figure 11. Predicted factor of safety against slip for the bedding plane at elevation 797: Option 1 model (upper left); Option 1' (upper center); Option 1A (upper right); Option 2 (lower left); Option 1B (lower center); and Option 1C (lower right).

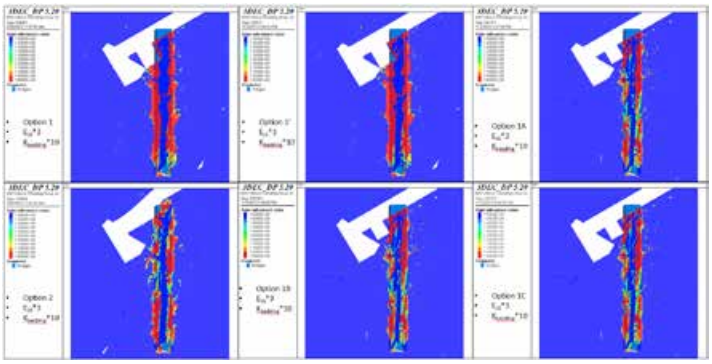

Figure 12. Predicted factor of safety against slip for the bedding plane at elevation 801: Option 1 model (upper left); Option 1' (upper center); Option 1A (upper right); Option 2 (lower left); Option 1B (lower center); and Option 1C (lower right).

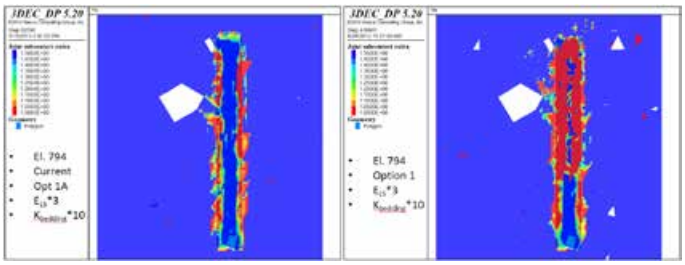

Figure 13. Comparison of factor of safety for the bedding plane at 794: current condition (left); Option 1 (right).

Option 1 is rated worse than the current condition for all bedding planes, as is Option 1'. Option 2 is rated better than the current condition, because the vertical loads from the transfer beam foundations add to the vertical stress on the bedding planes, providing clamping action and increased factor of safety. Option 1A is rated slightly worse for 789 and 794 bedding planes, and slightly better for 797 and 801 bedding planes. Options 1B and 1C are rated better for all bedding planes.

6.0 Summary and Conclusions

6.1 Summary

Itasca developed, calibrated, and applied a *3DEC* structural model of the Terminal 1-Lindbergh LRT station at Minneapolis-Saint Paul International Airport. The model included the soil, upper limestone, lower limestone and sandstone, existing and future excavations, rockbolt support, and future column loads. The limestone is modeled with four bedding planes at elevations 789, 794, 797, and 801. The limestone also includes a system of joints in three orientations and with different properties depending upon the observations made during construction. Model calibration identified three variations from the base case properties that most closely matched the displacements measured during construction. These three calibration cases were carried through to the model application phase.

6.2 Conclusions

1. Option 1 produces approximately a 50 percent increase in roof deflection compared to the current state. After application of the column loads, bedding plane slip and tension is widespread.
2. Option 2 produces approximately a 10 percent increase in deflection compared to the current state. After application of the column loads, bedding plane slip and tension is significantly less than Option 1.
3. Option 1' (Option 1 prime): Model results show that the Option 1' rockbolting has a limited effect on station roof displacements, while positively affecting the factor of safety against slip on bedding planes at 798 and 794.
4. Option 1A: Model results show that the displacement effects of the column loads is limited to about 75 ft in the vicinity of the loads. Factor of safety impacts for bedding planes at 798 and 794 are also limited to about 75 ft in the vicinity of the loads.
5. Option 1B: Model results show that the Option 1B rockbolting has a limited effect on station displacements, while positively affecting the factor of safety against slip on bedding planes at 798 and 794.
6. Option 1C: Model results show that displacement effects of column loads for Option 1C is less than either Option 1A or 1B. Factor of safety results are similar to the current state of the station for bedding planes 798 and 794.

6.3 Overall Conclusions

Options 2, 1', 1A, 1B, and 1C are considered to be geostructurally feasible. Option 1 is not considered to be feasible based on the current modeling results.

7.0 Acknowledgments

Itasca Consulting Group gratefully acknowledges the Metropolitan Airports Commission and Kimley-Horn and Associates, Inc., for funding this work and granting permission to publish. Itasca also gratefully acknowledges the assistance of CNA Consulting Engineers in providing historical information on station construction, instrumentation results, limestone jointing and bedding, previous modeling, and review of the *3DEC* model described herein.

Two USGS reports draw attention to 'unintended consequences' resulting from unconventional oil and gas extraction

Submitted by Bezalel Haimson,
Professor Emeritus, University of Wisconsin-Madison

Two recently released studies by the U.S. Geological Survey (USGS) reveal two major unintended consequences resulting, not directly from the successful unconventional oil and gas extraction techniques, but from their byproduct: the often toxic wastewater and its disposal deep underground.

The USGS report entitled "2016 One-Year Seismic Hazard Forecast for the Central and Eastern United States from Induced and Natural Earthquakes" (released March 28, 2016, and available online at *http://pubs.usgs.gov/of/2016/1035/ofr20161035.pdf),* highlights the recent earthquakes experienced in previously quiescent states such as Oklahoma, and makes predictions for future induced seismic hazards. Here are some excerpts from the report:

"Earthquake rates have recently increased markedly in multiple areas of the Central and Eastern United States (CEUS), especially since 2010, and scientific studies have linked the majority of this increased activity to wastewater injection in deep disposal wells... Between 1980 and about 2010, CEUS earthquake rates were relatively stable, but recent rates in some areas have increased by more than an order of magnitude. Such changes have caused concern to many, including residents, business owners, engineers, and public officials responsible for mitigating or responding to the effects of these earthquakes on nearby populations."

"The higher hazard levels in active injection areas could lead to potential damage across Oklahoma, Kansas, Colorado, New Mexico, Texas, and Arkansas. High hazard levels in some of these zones of induced seismicity are comparable with those in California and New Madrid, which also have high earthquake rates. Over the past decade, damage has already been observed at several locations in these states." However, the report concedes: "Uncertainties are high in this analysis, and an important topic for future research is to try to quantify and reduce these uncertainties."

A second USGS study, published on May 9, 2016 is entitled "Indication of Unconventional Oil and Gas Wastewaters Found in Local Surface Waters" (*http://toxics.usgs.gov/highlights/2016-05-09-uog_wastes_in_streams.html*). This study found evidence of Unconventional Oil and Gas (UOG) wastewaters in surface waters and sediments collected downstream from the disposal facility, specifically elevated concentrations of barium, bromide, iron, calcium, chloride, sodium, lithium, and strontium. Microbial communities in downstream sediments had lower diversity and shifts in community composition compared to upstream locations.

The study provides evidence of changes to stream chemistry and potential concerns for environmental health at sites where disposal facilities are located adjacent to streams. Although most of the chemical levels were not high enough to cause immediate and lethal concerns for aquatic life, the observed changes in the microbial community indicate potential adverse health outcomes for organisms living in or near the stream.